

Section 5

STUDIES OF CARBURIZATION, SWELLING AND PROMOTER DISTRIBUTION IN IRON CATALYSTS

5.1 Introduction

The properties of fully carburized iron Fischer-Tropsch catalysts have been the subject of several studies.^{1*} However the changes of the surface and bulk properties of the catalysts that accompany carburization in H₂/CO gas mixtures under specified conditions have received less attention. During carburization of iron, the bulk reactions lead to the formation of different iron carbides which can undergo further solid-phase reactions. Both classes of reactions are temperature dependent,¹⁻⁴ as summarized in Table 5-1. Our experiments were designed to examine the kinetics of carbon deposition, incorporation, and the development of ferromagnetic phases by simultaneous measurements of mass change and magnetic susceptibility during temperature-programmed and isothermal carburization. We have examined the magnetic properties of iron catalysts that ERDA-PERC had subjected to Fischer-Tropsch synthesis conditions.

5.2 Catalyst Samples

Samples of the iron catalysts B-2 and B-6 provided by ERDA-PERC were produced from a mixture of magnetite and the appropriate oxides, by calcining the mixture in an open iron crucible for 15 min in an induction furnace to 1740 to 1775 K.⁵ The chemical analyses of the catalysts after calcining are shown in Table 5-2. The most significant

*References for Section 5 are given on page 5.15.

difference between the catalysts in the high SiO₂ content in B-2. Most likely, the formation of iron silicate contributed to the high Fe²⁺/Fe³⁺ in B-2 as compared to B-6.

Two usual catalysts, Raney iron and Fused iron, provided by ERDA-PERC were also examined to determine their magnetic properties.

5.2.2 Magnetic Susceptibility Apparatus

To study simultaneously the rate of carbon buildup and the magnetic properties of the catalysts, we used a magnetic susceptibility apparatus equipped with an electronic microbalance (Cahn Model RS). We used a modified Faraday technique to measure magnetization where the vertical magnetic field gradient was provided by a set of electromagnetic gradient coils^{6,7} mounted on the flat pole faces of a 12-inch magnet. The assembly of the gradient coils, its power supply, and the hang-down tube with furnace for heating the sample in various gaseous atmospheres were purchased from George Associates (Berkeley, California). Two thermocouples were employed; one in the gas stream just below the catalyst sample to measure the catalyst temperature, and one near the furnace to control its temperature. The gradient coils were operated at a frequency of 5 cps, and all measurements were normalized to a coil current of 1.00A. The electrical signal from the microbalance was used to record mass changes and magnetization as a function of the magnetic field (0 to 8 kOe) or as a function of sample temperature (300 to 925 K), i.e., thermomagnetic analysis (TMA). For the TMA analysis, we used a lower field of 2.5 kOe to obtain more distinct Curie temperatures⁸ and to decrease the effects of the magnet on the microbalance. For recording the magnetization, a lock-in amplifier was used to convert the 5 cps component in the microbalance signal to a dc voltage.

Catalyst samples (30 mg) were placed in a small quartz container suspended from the microbalance by a quartz fiber. The system was

initially purged with helium ($100 \text{ cm}^3 \text{ min}^{-1}$) at room temperature. A separate stream of helium flowed continuously through the microbalance case. For reduction of the catalysts, we followed the procedure recommended by ERDA-PERC. First hydrogen flow ($100 \text{ cm}^3 \text{ min}^{-1}$) was established, then the temperature was programmed to rise at 18 K hr^{-1} from 450 to 725 K, and finally the sample was cooled in hydrogen. Changes in temperature and sample mass were recorded continuously during the reduction.

The reduced catalysts were carburized under either isothermal or temperature-programmed conditions at 1 atm. Unless otherwise stated, the carburizing gas was a mixture of H_2 and CO ($\text{H}_2/\text{CO} = 3$ by vol).

5.2.3 High Pressure Tubular Reactor

For high pressure carburization (1 to 10 atm) a tubular reactor was used. It was constructed of stainless steel (304 SS), with an internally mounted Pyrex glass frit to support the powdered catalyst and was designed so that the gas flowed into the reactor and through the catalyst bed before leaving the reactor. In a typical experiment, 0.090 g catalyst was loaded onto the glass frit of the high-pressure reactor. The sample was reduced in flowing H_2 (space velocity of $2 \times 10^4 \text{ hr}^{-1}$) at 1 atm while the temperature was raised linearly from 450 to 725 K over a 16-hr period. The catalyst was subsequently cooled to 450 K and exposed to a flowing stream of $\text{H}_2/\text{CO} = 3/1$ (space velocity of $5 \times 10^5 \text{ hr}^{-1}$) at 1 or 10 atm while the temperature was programmed to rise from 450 to 575 K at a linear rate of 0.62 or 0.90 K min^{-1} . The catalyst was then cooled to room temperature in syngas and removed for analyses by TMA, x-ray, and Auger electron spectroscopy (AES).

5.2.4 Catalytic Measurement

Surface reactivity of the Fischer-Tropsch catalysts and carbon buildup were evaluated in two different experimental systems. One system, consisting of a microreactor, was used in a continuous flow (15 psi) mode. In this system, the catalyst (0.5 g) was reduced in H_2 (15 hr at 623 K followed by 2 hr at 723 K) and then exposed to a carburizing gas (H_2/CO or He/CO) at 1 atm. Product content was determined by gas chromatographic analysis on a temperature-programmed silica-gel column. The other system made use of the temperature programmed surface reaction (TPSR) technique. In that system, the catalyst was reduced as before in a microreactor, flushed with He, exposed to known amounts of CO, again flushed with He, and then to flowing H_2 while the temperature of the catalyst was raised at a prescribed linear rate from 293 to 770 K. The effluent from the reactor was sampled by a mass spectrometer, which rapidly and repetitively scanned through the mass range from C_1 to C_9 hydrocarbons.


5.2.5 Gas Purification

The CO (Matheson "Ultra-pure" 99.8%) was rid of iron carbonyl by passing the sample through a copper tube packed with 1/8-inch Kaiser Al_2O_3 spheres and copper turnings and cooling it in a bath of dry ice and acetone. Hydrogen and helium (Matheson, prepurified) were passed through traps in liquid nitrogen.

5.3 Results

5.3.1 Hydrogen Reduction

Mass losses during reduction of catalysts B-2 and B-6 at atmospheric pressure were less than the theoretical values for complete



reduction of the iron to the metallic state on the basis of the catalyst composition (Table 5-2). The results suggest that reduction of B-2 was less complete than B-6, possibly due to the presence of iron silicate.

Also listed in Table 5-2 are the saturation magnetization values measured for these catalysts. After reduction, the magnetization was much lower for catalyst B-2 than for B-6. Thermomagnetic analysis (TMA) identified magnetite as the only ferromagnetic phase in the unreduced catalyst, and iron in the reduced samples.

5.3.2 Mass Increase Resulting from Carburization

The increase of mass of catalyst B-6 during a 72-hr carburization experiment under partial nonisothermal conditions is shown in Figure 5-1. During the first 4 hr the temperature was programmed to rise from 425 to 598 K at a constant heating rate, after which it was held constant at 598 K.

An additional series of measurements were carried out under isothermal conditions at 1 atm (Figure 5-2). For these experiments, carburization was limited to a period less than 6 hr. The data, analyzed in terms of the parabolic rate law, exhibit two distinct regions of carburization (Figure 5-3). The parabolic rate constants have been calculated from the initial and final slopes (Table 5-3). The parabolic rate constants yield the activation energies and preexponential factors summarized in Table 5-4.

5.3.3 Magnetization Resulting from Carburization

TMA measurements were made after isothermal carburization and after temperature-programmed carburization of catalysts B-2 and B-6. For these TMA analyses, we replaced the flowing syngas by helium and lowered the temperature from the reaction temperature to 350 K. From

the Curie temperatures so evaluated, we assigned specific ferromagnetic phases in accordance with published data (Table 5-5). The fraction of the total magnetization force due to a given phase was estimated by extrapolating the TMA curve of a given ferromagnetic phase to 300 K. The procedure for this estimation is illustrated in Figure 5-4 for TMA curves of carburized catalyst B-6 ($H_2/CO = 1.5$, 573 K, 4 hr). We obtained the upper TMC curve by raising the temperature of the sample from 350 to 950 K, and the lower curve, by then lowering the temperature from 950 to 350 K.

The difference in the TMA curves can be accounted for by a reaction above 650 K between Fe_2C and Fe that resulted in formation of Fe_3C . Therefore, when this reaction can occur, it is necessary to limit the TMA to temperatures less than 650 K. In any case, the relative magnetization due to the various ferromagnetic phases can only be semi-quantitatively estimated because of the unknown domain size of the ferromagnetic phases.

The changes in the ferromagnetic phases during the 72-hr carburization of catalyst B-6 (Figure 5-5) were measured by TMA at the times indicated in Figure 5-1. As the α -Fe phase decreased, the Fe_2C (Hagg) phase increased, and the Fe_3C (cementite) phase exhibited a transient existence reaching a maximum at about 5 hr.

For the isothermal carburization of catalysts B-2 and B-6, the TMA results (Table 5-6) exhibit the following trends:

- For a given carburization temperature the total magnetization force was much greater for catalyst B-6 than for B-2
- With increasing temperature the fractional contribution to the total magnetization by hexagonal, close-packed (hcp) Fe_2C and α -Fe decreased and that by

Fe_2C (Hagg) increased. This latter effect is due to the higher stability of Hagg carbide over hcp Fe_2C , as confirmed in a separate isothermal carburization of catalyst B-6 at 598 K. After a weight gain of 2.5 and 4.5 wt% TMA revealed only Fe_2C (Hagg), not Fe_2C (hcp) nor Fe_3C .

In the carburized catalysts, another ferromagnetic component, with a Curie temperature at about 423 K, was present. This component is probably associated with the $\text{K}_2\text{O}\cdot\text{Fe}_2\text{O}_3$ phase.¹ Its magnetization was small, about 3 to 6% of the total, and its contribution was not included in the data in Table 5-6.

The effect of heating rate during carburization ($\text{H}_2/\text{CO} = 3/1$) on the magnetic properties of the catalysts were studied at 1 atm in the magnetic susceptibility apparatus and in the tubular reactor (Table 5-7). The mass gain of the samples carburized at 1 atm in the susceptibility apparatus was 6.5 ± 0.2 wt%. To examine in more detail the effect of pressure on the formation of different bulk phases during carburization at a constant heating rate ($0.62 \text{ K}\cdot\text{min}^{-1}$) we performed additional experiments in the tubular reactor (Table 5-8). The TMA results indicate that

- The total magnetization increased with heating rate
- Fe_2C (Hagg) was the dominant ferromagnetic phase above 573 K
- At comparable heating rates catalyst B-6 exhibited greater magnetization than did B-2
- Fe_2C (hcp) was observed only in catalyst B-2
- For a given catalyst, the carburization pressure had a negligible effect on the relative amounts of the ferromagnetic phases produced.

The Curie temperature of a ferromagnetic phase which we assigned to Fe_2C (Hagg) varied from 520 to 617 K (Table 5-7), although published data indicate a range of 520 to 549 K (Table 5-5). The highest values of the Curie temperature for Fe_2C (Hagg) were obtained by carburizing in the tubular reactor. Also, in some instances the Curie temperature measured from Fe_2C (hcp) was higher than the reported value of 653 K. Therefore, the Curie temperature appears to be affected by the catalyst composition and by the heating rate during carburization. These effects, then, determine the actual catalyst temperature.

5.3.4 Effect of Carburizing Gas Composition

After reduction in hydrogen, catalyst B-6 was carburized at several temperatures in a gas containing various H_2/CO ratios, and the bulk phases were determined by x-ray diffraction and TMA. Carburization at 673 K was carried out in the tubular reactor. The bulk phase composition depended both on gas composition and temperature (Table 5-9). Fe_3C (cementite) predominated when catalyst B-6 was exposed to CO, whereas when it was exposed to H_2/CO mixtures, Fe_2C (Hagg) was the major phase. Larger mass increases were observed at higher temperatures in gas mixtures of H_2 and CO.

5.3.5 Magnetic Properties of Fischer-Tropsch Catalysts Carburized at ERDA-PERC

Thermomagnetic analysis results for the Raney iron and Fused iron catalysts provided by ERDA-PERC (Table 5-10) show that

- The total magnetization was much greater for Fused iron than for Raney iron
- The major ferromagnetic component in both catalysts was Fe_3O_4 (magnetite) (X-ray diffraction analysis confirmed the presence of only Fe_3O_4 for the Fused iron catalyst exposed to syngas for 72 hr)

- α -Fe decreased with exposure to syngas
- Fe_2C (Hagg) was present only in the Raney iron sample.

5.3.6 Relationship Between Magnetization and Mass Increase During Carburization

The relationship between total magnetization and mass increase was investigated during isothermal (598 K) carburization ($\text{H}_2/\text{CO} = 3/1$) of reduced catalyst B-2. The results are summarized in Figure 5-6 in which the mass increase identified by the carbon/iron atom ratio is indicated on the abscissa, and the percent of the initial magnetization force due to α -Fe at 598 K is plotted on the ordinate. Since the reaction temperature is above the Curie temperatures of Fe_2C (Hagg) and Fe_3C and Fe_2C (hcp) are unstable at this temperature, the magnetization measured was due almost exclusively to α -Fe. The experimental points appear to follow two lines with different slopes (Figure 5-6) whose intercepts with the abscissa correspond to a carbon/iron ratio $\text{C}/\text{Fe} = 1/8$ and $\text{C}/\text{Fe} = 1/2.2$.

5.3.7 Chemical Activity of Surface Intermediates

In conjunction with the magnetic studies described above, we also studied catalyst B-6. Our purpose was to measure steady-state catalyst activity and to identify the buildup of carbon-containing intermediate species on the surface of the catalyst by exposing the catalyst to pulses of hydrogen after different degrees of carburization in H_2/CO mixtures (3/1 by volume) and in CO. Initially, the product stream was found to contain CO_2 , CH_4 , C_2H_4 , C_2H_6 , C_3H_6 , and some higher molecular-weight hydrocarbons, some of which condensed at the exit from the reactor. CO conversion was nearly constant at a level of about 35 vol%.

The catalyst swelled markedly when carburized in $H_2/CO = 3/1$ at 673 K. At the same time, the CO consumption rose to 100%. Under these conditions, the product composition had changed to CH_4 , CO_2 , C_2H_6 , and C_3H_8 (in order of decreasing yield). The production of olefins and higher molecular weight hydrocarbons appeared to have ceased. For catalysts B-6 carburized at 673 K, the product distribution as a function of reaction temperature is given in Figure 5-7. Although CO_2 formation shows little change with temperature, the production of C_1 - to C_3 -hydrocarbons exhibited maxima near 623 K for CH_4 and near 573 K for C_2H_6 and C_3H_8 .

Catalyst B-6 when carburized in CO/He mixtures (rather than H_2/CO) at 673 K did not "swell". When B-6 was exposed to H_2 pulses, methane was the only product observed. CO-adsorption measurements at 298 K show that the freshly reduced catalyst B-6 adsorbs 2.76×10^{-6} moles of CO per gram of catalyst. However the "swelled" catalyst formed by carburization in $H_2/CO = 3/1$ did not adsorb CO.

5.3.8 AES Study of Promoter Distribution

Small quantities of alkali metal oxides have long been known to act as promoters in iron-based Fischer Tropsch catalysts, but the mechanism of promoter action is not established. The relative quantity of promoter in the bulk may differ significantly from that at the surface, where the catalytic reactions occur. Thus, we conducted a series of AES measurements on potassium-promoted, iron-based Fischer-Tropsch catalysts to characterize the distribution of promoter between surface and bulk, and to identify the effect of chemical reaction on the distribution.

AES reveals the elemental components in a surface layer, generally less than 20 \AA . Hence, sequential analyses of a region from which

material is being continuously etched by Ar^+ ion bombardment produce a depth profile with a resolution approaching atomic dimensions. We have obtained such AES depth profiles for catalyst B-6 pretreated in several different ways. The results are described below.

Catalyst B-6 contained 0.27 wt% K_2O in bulk, but in the fresh catalyst the potassium was so highly segregated near the surface that it comprised nearly 40 at.% of the surface layer (Figure 5-8). The relative concentration of potassium diminished with depth,^{*} whereas that of iron increased. Carburization caused the potassium concentration at the surface to diminish, particularly on a catalyst surface carburized in pure CO (Figure 5-9). The relative concentration profile of potassium beneath the surface was similar in both the fresh and the carburized catalyst (Figure 5-10). Potassium was completely absent from the surface of samples of the carburized catalyst and was not detectable at depths^{*} greater than 1000 Å. On the carburized catalyst, surface carbon extended into the bulk of the catalyst, particularly in the sample exposed to syngas for 5 hr at 673 K. This exposure caused the catalyst to swell considerably.

The AES examination also provides some chemical information concerning the surface components. Specifically, the narrower electronic states in the valence band of carbon when combined as a metal carbide relative to those in graphite or amorphous carbon produce added peaks in the KVV spectrum. Unfortunately, this fine structure is obliterated by the strong LMM potassium peaks, but on potassium-free samples we

* We did not calibrate the Ar^+ ion sputtering rate for these catalysts. Based on measurements under similar conditions with other materials, we estimate the sputtering rate to be approximately 7 \AA min^{-1} . Also we did not attempt to correct our data for variation in the individual sputter yields of the various components in the catalyst. Consequently, the depth profiles are measurements of trends in the relative concentration of the components with depth.

could identify the state of the carbon as graphitic and not carbidic (Table 5-11). The MVV spectrum of iron also offers some chemical information (Table 5-11). The oxidation of a metallic iron surface caused a shift in the $M_{2,3}VV$ peak from 46 to 42 eV.⁹ Hence, we were able to identify the presence of iron oxide and/or metallic iron in the catalyst surfaces.

5.4 Discussion

5.4.1 Carburization Kinetics

The trends in the mass increase during carburization of reduced B-2 and B-6 catalysts (Figure 5-1) are qualitatively similar to those reported.^{1,3,10} The rapid initial mass gain, presumably due to carbide formation, is followed by a lower, constant rate of increase that is attributed to free carbon.³ The formation of the free carbon has been associated with catalyst swelling, which occurred only on exposure to H_2/CO mixtures and when the Fe_2C (Hagg) phase predominated.

Information on the mechanism of carburization can be obtained from the mass increase observed under conditions of isothermal carburization. The parabolic rates observed (Figure 5-3) suggest that carburization proceeded in two distinct diffusion-limited regimes. The observation of two diffusion-controlled regimes is supported by the combined study of mass increase and magnetization during carburization (Figure 5-6). The intercept corresponding to the Fe/C ratio of 8 suggests a dilute phase of iron carbide in iron. The intercept at Fe/C = 2.2 is close to the value expected for Fe_2C (Hagg), the predominant ferromagnetic phase in this sample after carburization.

To account for the carburization of iron we propose the following four-step mechanism:

- (1) Dissociative chemisorption of CO
- (2) Bulk diffusion of carbon resulting in dilute phase of iron carbide in Fe during the initial parabolic regime
- (3) Further bulk incorporation of carbon resulting in the formation of iron carbides during the latter parabolic regime
- (4) Buildup of free surface carbon.

The rates of these various steps will depend on carburization conditions and catalyst composition. That the activation energy for mass increase during carburization is higher for catalyst B-2 than for B-6 (Table 5-4) may be associated with the greater amount of SiO_2 in B-2.

Carbon buildup at 598 K became clearly evident when the bulk composition attained Fe_2C , mostly Hagg carbide. Similar behavior was observed by Storch et al.,¹ who reported that the amount of carbidic carbon became constant after carburizing in 0.1 atm CO at 598 K for 3 hr, and by Hofer et al.¹⁰ during carburization in CO at lower temperatures. Turkdogan and Vinter¹¹ studied carburization of iron in CO and H_2/CO mixtures, mainly at 873 K. They reported that the rate of carbon deposition increased with temperature in the range of 673 to 1073 K and that the carbon deposition ceased when the iron was converted to cementite.

5.4.2 Ferromagnetic Phases

Our TMA results indicate that the ferromagnetic phases produced by carburizing the iron catalysts depend primarily on carburization temperature (Table 5-1) and, to some extent, on the H_2/CO ratio. When carburizing in $\text{H}_2/\text{CO} = 3/1$ with increasing temperature, we observed the following:

- α -Fe decreased
- Fe_2C (hcp) increased, but above 573 K it was unstable with respect to Fe_2C (Hagg), which was the predominant phase at carburization temperatures up to 598 K
- Fe_3C (cementite) was produced under special conditions.

At the highest temperature (673 K), Fe_3C formation was favored by carburizing in CO, but Fe_2C (Hagg) was favored when both H_2 and CO were present (Table 5-9). Also, Fe_3C was formed and then disappeared in the 72-hr carburization experiment (Figure 5-5). The transitory formation of Fe_3C has been reported previously.¹²

The large range of Curie temperatures exhibited by our carburized B-6 catalysts (520 to 617 K) and the total magnetization appear to be associated with the thermal history of the sample, especially the heating rate during carburization. The data indicate that low Curie temperature and high magnetization accompany high heating rates. This effect may be associated with the higher temperatures attained by the catalyst at large heating rates. Under these conditions, the exothermic heat of the carburization reaction cannot be as readily dissipated from the sample to the environment. Similarly, the lower Curie temperatures of the Fe_2C (Hagg) (520 to 570 K) produced by carburizing in the magnetic susceptibility apparatus relative to the tubular reactor (598 to 617 K) may be the result of faster heat transfer from the catalyst in the tubular reactor (Table 5-2).

The variable Curie temperatures observed in our study can probably be ascribed to a single phase with variable degrees of crystalline imperfection. At high heating rates during carburization, the resulting high catalyst temperatures favored annealing of crystallite imperfections and an increase in the size of ferromagnetic domains, which in turn resulted in greater magnetization. Three ferromagnetic phases in

carburized iron have been reported to have Curie temperatures in the range of 520 to 653 K. Two modifications of Hagg Fe_2C carbides were characterized by x-ray diffraction with Curie temperatures from 513 to 523 K and 533 to 543 K.² The third ferromagnetic phase is the well-characterized hexagonal Fe_2C with a Curie temperature of 653 K. To account for the existence of two modifications of Hagg Fe_2C , Cohn et al.²¹ suggested differences in crystalline imperfections resulting from small crystallites or lattice strain.

The minor ferromagnetic phase that was evident in some samples from the Curie temperature of 423 K was assumed to be due to potassium ferrite, $\text{K}_2\text{O}\cdot\text{Fe}_2\text{O}_3$, ($\theta = 423 \text{ K}$).³ The amount of this phase indicates that the K_2O that was added as a promoter is mostly tied up with an iron oxide.

5.4.3 Ferromagnetic Process in Catalysts Used in Synthesis at ERDA-PERC

TMA of the catalysts used at ERDA-PERC indicated a different ferromagnetic composition than that observed for the catalysts B-2 and B-6 carburized in our laboratory. In particular the catalysts carburized at ERDA-PERC contained smaller amounts of Fe_2C (Hagg) and large amounts of Fe_3O_4 (magnetite). These results are in agreement with reported compositional changes of iron Fischer-Tropsch catalysts during operation in syngas.^{1,13} The amount of Hagg Fe_2C remains almost constant after the initial carburization (e.g., after about 100 hr), and the magnetite increases slowly over the period of many hundreds of hours. Thermodynamically, the formation of Fe_3O_4 is favored under Fischer-Tropsch conditions (see Section 6).

5.5 References

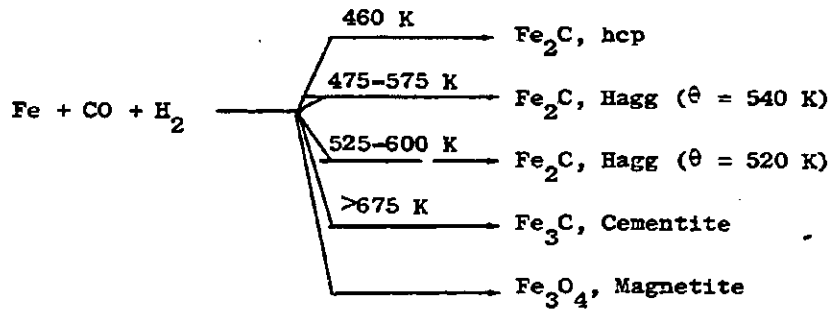
1. H. H. Storch, N. Columbic, and R. B. Anderson, "The Fischer-Tropsch and Related Syntheses," (Wiley, New York, 1951).

2. E. M. Cohn, E. H. Bean, M. Mentser, L.J.E. Hofer, A. Pontello, W. C. Peebles, and K. H. Jacks, *J. Appl. Chem.*, 5, 418 (1955).
3. H. Pichler and H. Merkel, "Chemical and Thermomagnetic Studies on Iron Catalysts for Synthesis of Hydrocarbon," U.S. Bureau of Mines, Technical Paper 718, (1949).
4. E. C. Stoner, "Magnetism and Matter," (Methuen and Co., London, 1934), pp. 280-434.
5. Memo to B. B. Blaustein, PERC from J. E. Mauser, Bu. of Mines, Albany Metallurgy Research Center, April 18, 1975.
6. R. T. Lewis, *Rev. Sci. Instru.*, 42, 31 (1971).
7. R. T. Lewis, *J. Vac. Sci. Technol.*, 11, 404 (1974).
8. A. Kussman and A. Schulze, *Physik, Z.* 38, 42 (1937).
9. M. Suleman and E. B. Pattinson, *Surface Sci.*, 35, 75 (1973).
10. L.J.E. Hofer, A. M. Cohn, and W. C. Peebles, *J. Am. Chem. Soc.*, 71, 189 (1949).
11. E. T. Turkdogen and J. V. Vinters, *Metallurgical Trans.* 5, 11 (1974).
12. H. Pichler and H. Schulz, *Chemie Ing. Techn.*, 42, 1162 (1972).
13. R. B. Anderson, L.J.E. Hofer, E. M. Cohn, and B. Seligman, *J. Am. Chem. Soc.* 73, 944 (1951).

Table 5-1

PRINCIPAL CARBURIZATION REACTIONS OF
IRON AND PHASE CHANGES

CARBURIZATION REACTIONS



PHASE CHANGES

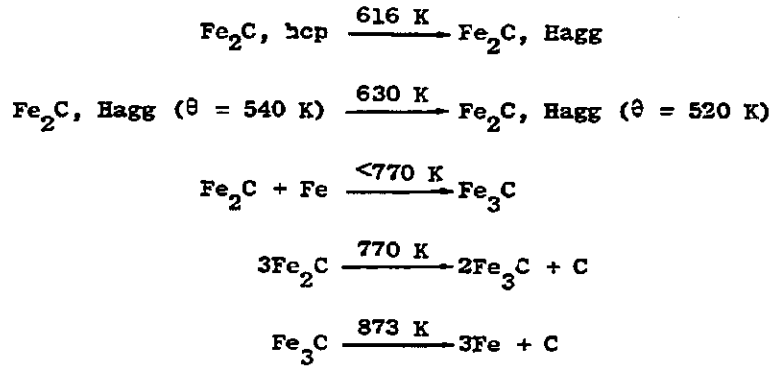


Table 5-2

PROPERTIES OF IRON OXIDE
CATALYSTS B-2 AND B-6

Property	Catalyst	
	B-2	B-6
Analysis (wt%) ^a		
Fe (total)	63.0	71.9
Fe ⁺²	59.0	29.5
Fe ⁺³	3.6	41.6
SiO ₂	4.41	0.09
MgO	1.07	0.95
K ₂ O	0.36	0.27
H ₂ Reduction (wt%) ^b		
Mass Loss	19.0	21.9
Expected ^c	31.2	26.8
Apparent Saturation Magnetization Force ^d at 300 K (dynes g ⁻¹ sample)		
Before reduction	e	240
After reduction	19	450

^aAfter calcination at 1740 to 1779 K (chemical analyses provided by ERDA-PERC)

^bIn 1 atm. H₂, heated from 450 to 725 K at 18 K hr⁻¹

^cBased on total Fe

^dMagnetic field = 7 kG

^eNot measured

Table 5-3

PARABOLIC RATE CONSTANTS FOR ISOTHERMAL
CARBURIZATION OF CATALYSTS B-2 AND B-6

Catalyst	Carburizing Temperature ^a (K)	Parabolic Rate Constant (wt% min ^{-1/2})	
		Initial Slope	Final Slope
B-2	481	0.15	-
	573	0.78	0.20 ± 0.02
	598	1.85	0.22
B-6	473	0.28	0.23
	523	0.48	0.29
	573	0.65	0.41
	597	0.72	-

^aCarburization in H₂/CO (3/1) at 1 atm

Table 5-4

ACTIVATION ENERGY AND PREEXPONENTIAL
FACTOR FOR MASS GAIN DURING ISOTHERMAL
CARBURIZATION OF CATALYSTS B-2 AND B-6

Catalyst	Slope ^a	Activation Energy (kcal mole ⁻¹)	Preexponential Factor (wt% min ^{-1/2})
B-2	Initial	10.8 ± 1.2	1.3 (+ 0.2) × 10 ⁴
	Final	-	-
B-6	Initial	4.2 ± 0.3	26 ± 2
	Final	3.2 ± 0.4	7 ± 1

^aSee Table 5-2 for conditions.

Table 5-5

CURIE TEMPERATURES OF FERROMAGNETIC
PHASES OF IRON AND COMPOUNDS

Phase	Curie Temperature (K)	References
$K_2O \cdot Fe_2O_3$	423	14
Fe_3C (Cementite)	478-493	14,16
Fe_2C (Hagg)	520-540	14,15
Fe_2C (hcp) ^a	653	14
Fe_3O_4 (Magnetite)	838-868	14,17
α -Fe	1041	14

^aHexagonal close-packed

Table 5-6

THERMOMAGNETIC ANALYSIS OF CATALYSTS B-2 AND B-6
AFTER SHORT-TERM ISOTHERMAL CARBURIZATION

Catalyst	Carburization ^a Temperature (K)	Magnetic Properties			
		Total Magnetization Force, M (dyne g ⁻¹)	Ferromagnetic Phases, Fraction of M (%)		
			Fe ₂ C (Hagg)	Fe ₂ C (hcp)	α-Fe
B-2	481	100	0	50	50
	573	27	93	0	7
	598	56	89	0	11
B-6	473	340	0	59	41
	523	380	45	45	10
	573	495	87	0	13
	598	285	95	0	5

^a Carburization in H₂/CO (3/1) at 1 atm.

Table 5-7

EFFECT OF HEATING RATE ON MAGNETIC PROPERTIES
OF CATALYSTS B-2 AND B-6 DURING CARBURIZATION IN $H_2/CO = 3/1$ AT 1 ATMOSPHERE

Catalyst	Heating Rate ^a (K min ⁻¹)	Total Magnetization Force, M (dyne g ⁻¹)	Magnetic Properties							
			Ferromagnetic Phases				α-Fe			
			Fe ₂ C (HCP)		Fe ₂ C (hcp)		Curie Temperature (K)		Fraction of M (%)	
			Curie Temperature (K)	Fraction of M (%)	Curie Temperature (K)	Fraction of M (%)	Curie Temperature (K)	Fraction of M (%)	Curie Temperature (K)	Fraction of M (%)
B-2	0.42	61	556	61	685	26	b	10		
	0.62	196	570	63	679	20	b	13		
	0.62 (T) ^a	180	598	70	630	17	b	14		
B-6	0.37	72	549	58	-	0	b	38		
	0.55	670	544	67	-	0	b	27		
	1.00	830	520	94	-	0	b	6		
	0.62 (T) ^a	350	617	87	-	0	b	13		

^a Carburization performed in magnetic susceptibility apparatus except for two runs in the tubular reactor (T).

^b Curie temperature of Fe is above maximum temperature of TMA.

^c Held at 575 K for 1.5 hr.

Table 5-8

EFFECT OF PRESSURE OF $H_2/CO = 3/1$ DURING TEMPERATURE-PROGRAMMED CARBURIZATION OF CATALYSTS B-2 AND B-6 ON MAGNETIC PROPERTIES

Catalyst	Total Gas Pressure ^a (atm)	Total Magnetic Force, M (dyne g^{-1})	Magnetic Properties							
			Ferromagnetic Phases						α -Fe	
			Fe ₂ C (Hagg)		Fe ₂ C (hcp)		Curie Temperature (K)	Fraction of M (%)	Curie Temperature (K)	Fraction of M (%)
			Curie Temperature (K)	Fraction of M (%)	Curie Temperature (K)	Fraction of M (%)				
B-2	1	180	598	70	630	16	b	14		
	10	175	617	69	662	17	b	14		
B-6	1	400	617	87	-	0	b	13		
	10	170	609	86	-	0	b	14		

^a Carburization in tubular reactor; temperature programmed at 0.62 K min^{-1} from 465 to 575 K.

^b Curie temperature of Fe above maximum temperature of TMA.

Table 5-9

EFFECT OF H₂/CO RATIO DURING CARBURIZATION AT
1 ATMOSPHERE ON MAGNETIZATION OF CATALYST B-6

H ₂ /CO Ratio (vol%)	Carburization			Total Magnetization Force, M (dyne g ⁻¹)	Magnetic Properties		
	Temperature (K)	Time (hr)	Mass Increase (%)		Fe ₃ C	Fe ₂ C (Hagg)	α-Fe
0 ^a	673 ^b	0.6	- ^c	-	100 ^d	0	0
1.5	573	4.0	7.8	590	10	63	27
3.0	573	3.8	7.4	400	0	87	13
	673 ^b	6.0	44 ^e	-	10	90 ^f	0
4.0	573	4.6	5.3	515	13	73	14
	600	4.2	9.1	480	36	54	10

^a He/CO = 1/1 (by vol)

^b Carburized in tubular reactor

^c Mass change not measured; catalyst did not swell

^d X-ray analysis indicates Fe₃C (cementite) only

^e Catalyst swelled in volume

^f X-ray analysis indicates Fe₂C (Hagg) and carbon as major phases

Table 5-8

EFFECT OF PRESSURE OF H₂/CO = 3/1 DURING TEMPERATURE-PROGRAMMED CARBURIZATION OF CATALYSTS B-2 AND B-6 ON MAGNETIC PROPERTIES

Catalyst	Total Gas Pressure ^a (atm)	Total Magnetic Force, M (dyne g ⁻¹)	Magnetic Properties					
			Ferromagnetic Phases					
			Fe ₂ C (Hagg)		Fe ₂ C (hcp)		α-Fe	
		Curie Temperature (K)	Fraction of M (%)	Curie Temperature (K)	Fraction of M (%)	Curie Temperature (K)	Fraction of M (%)	
B-2	1	180	598	70	630	16	b	14
	10	175	617	69	662	17	b	14
B-6	1	400	617	87	-	0	b	13
	10	170	609	86	-	0	b	14

^a Carburization in tubular reactor; temperature programmed at 0.62 K min⁻¹ from 465 to 575 K.

^b Curie temperature of Fe above maximum temperature of TMA.

Table 5-9

EFFECT OF H₂/CO RATIO DURING CARBURIZATION AT
1 ATMOSPHERE ON MAGNETIZATION OF CATALYST B-6

H ₂ /CO Ratio (vol%)	Carburization		Total Magnetization Forco, M (dyne g ⁻¹)	Magnetic Properties		
	Temperature (K)	Time (hr)		Mass Increase (%)	Ferromagnetic Phases, Fraction of M (%)	
				Fe ₃ C	Fe ₂ C (Hagg)	α-Fe
0 ^a	673 ^b	0.8	- ^c	100 ^d	0	0
1.5	573	4.0	7.8	10	63	27
3.0	573	3.8	7.4	0	87	13
	673 ^b	6.0	44 ^e	10	90 ^f	0
4.0	573	4.5	5.3	13	73	14
	600	4.2	9.1	36	54	10

^a He/CO = 1/1 (by vol)^b Carburized in tubular reactor^c Mass change not measured; catalyst did not swell^d X-ray analysis indicates Fe₃C (cementite) only^e Catalyst swelled in volume^f X-ray analysis indicates Fe₂C (Hagg) and carbon as major phases

Table 5-10

THERMOMAGNETIC ANALYSIS OF RANEY AND FUSED IRON
 CATALYSTS CARBURIZED IN H₂/CO (3/1) AT 10 ATMOSPHERE

Catalyst	Total Exposure To Syngas (hr)	Magnetic Properties			
		Total Magnetization Force, M (dynes g ⁻¹)	Ferromagnetic Phases Fraction of M (%)		
			Fe ₃ O ₄	Fe ₂ C (Hagg)	α-Fe
Raney iron	48-72	0.65	69	23	8
Fused iron ^a	3	10	55	0	45
	48-72	280	100 ^b	0	0

^a Sample CCI-C73-2-01

^b Phase confirmed by x-ray diffraction

Table 5-11

CHEMICAL STATE OF Fe and C IN
FISCHER-TROPSCH CATALYST B-6

Catalyst Treatment ^a	Carbon State	Iron State
None (fresh) (Figure 5-8)	Carbon absent	Mixed iron oxide and metallic iron throughout profiled region
H ₂ /CO = 3/1, 3 hr at 573 K (Figure 5-9)	b	Iron oxide at outer-surface changing to metallic iron with increasing depth
CO, 1 hr at 673 K (Figure 5-9)	b	Same
H ₂ /CO = 3/1, 1 hr at 673 K	Graphitic	Metallic iron
H ₂ /CO = 3/1, 5 hr at 673 K	Graphitic	Metallic iron

^aCarbon KVV fine structure obscured by strong potassium peak.

^bPrior to carburization the catalysts were reduced in H₂.

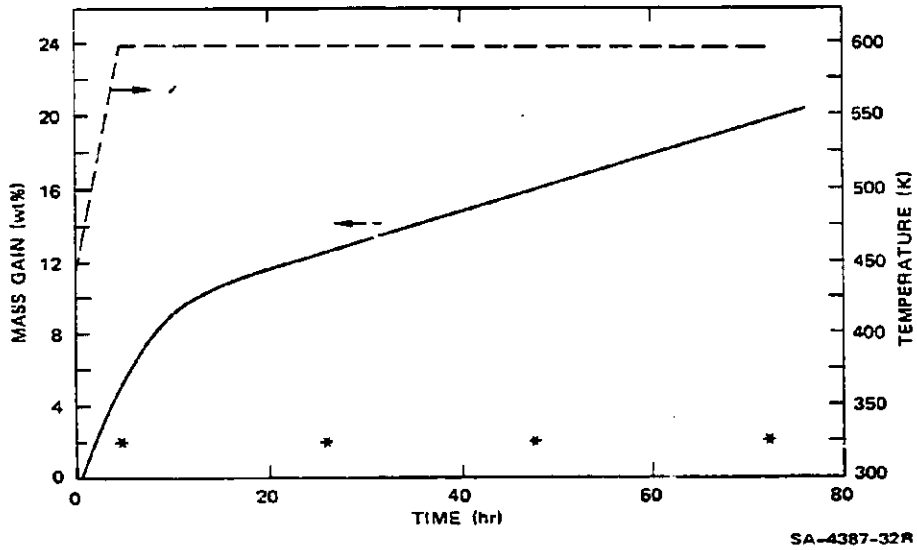
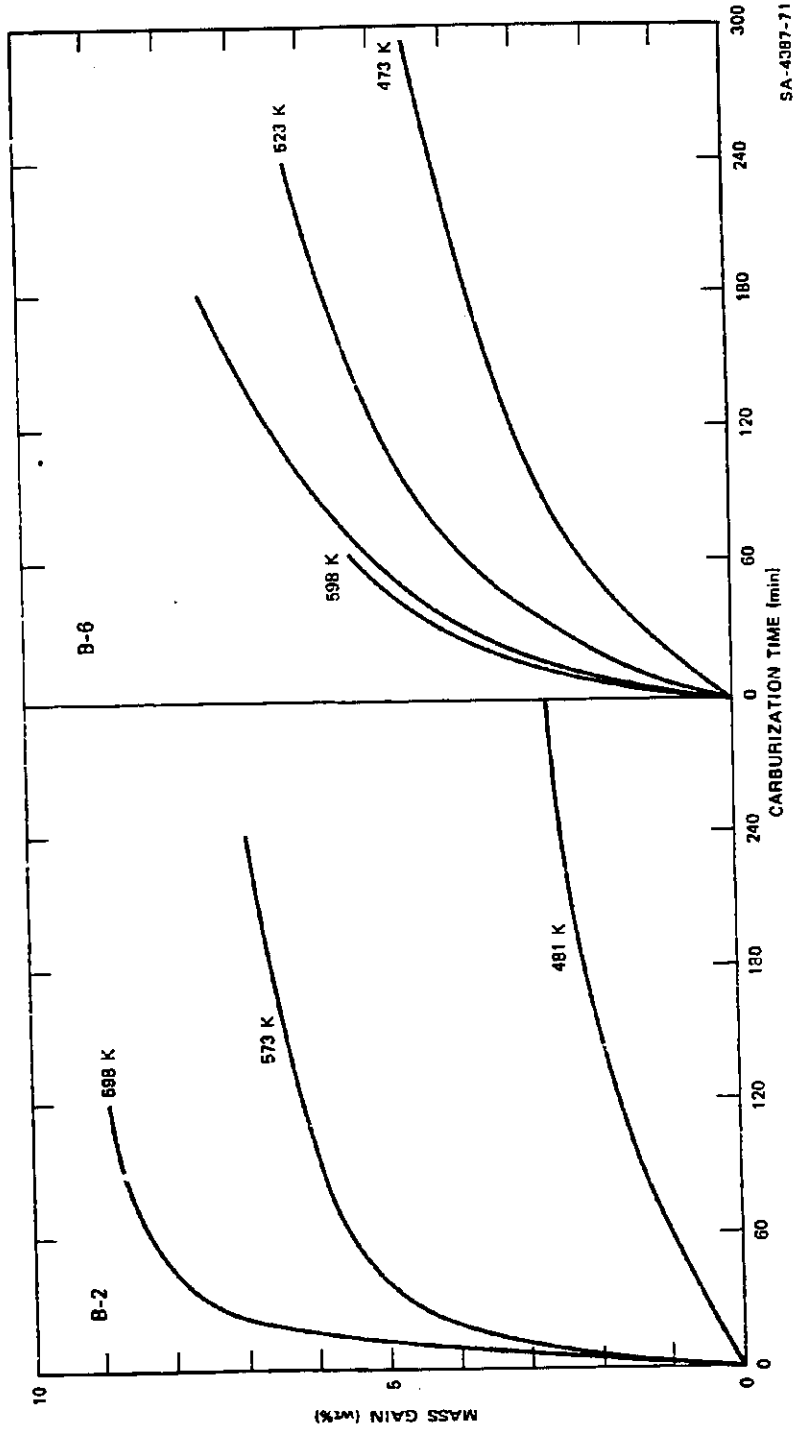


FIGURE 5-1 MASS GAIN DURING CARBURIZATION OF CATALYST B-6 IN H₂/CO (3/1) AT 1 atm
 Asterisk (*) indicates time at which thermomagnetic analysis was made.



SA-4087-71

FIGURE 5-2 MASS GAIN DURING ISOTHERMAL CARBURIZATION OF CATALYSTS B-2 AND B-6 IN H₂/CO (3/1) AT 1 atm

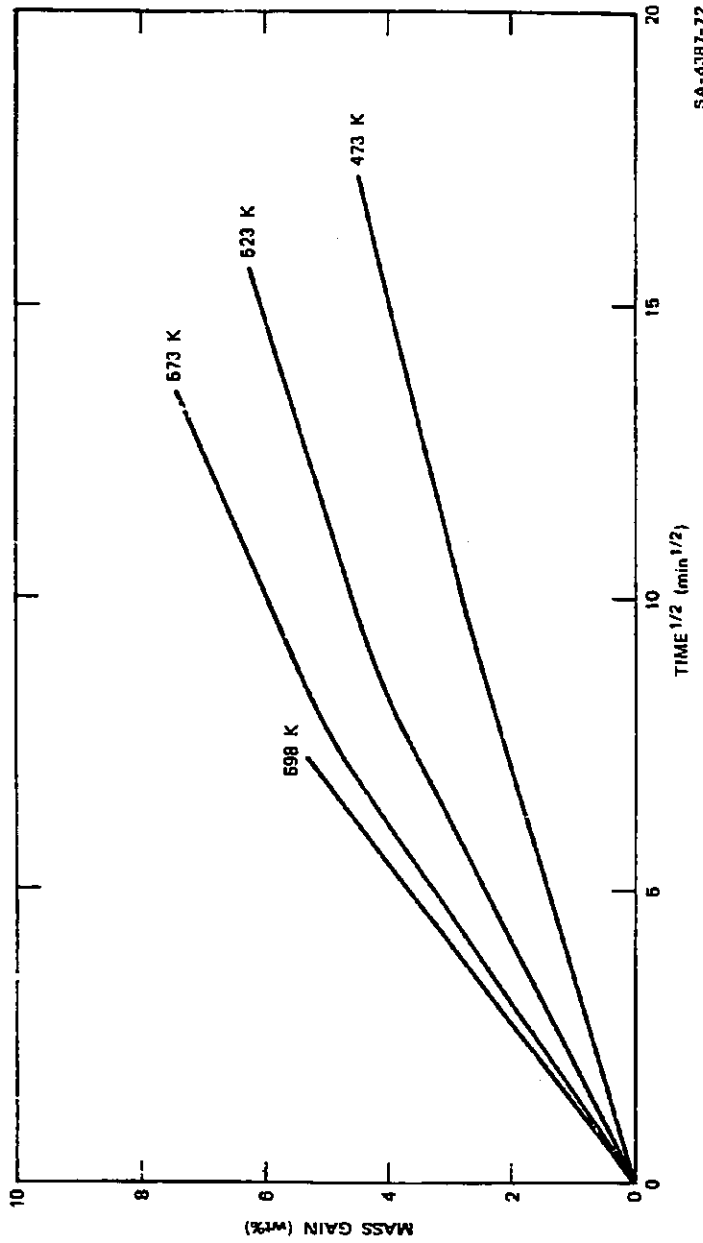


FIGURE 5-3 PARABOLIC RATE PLOT OF MASS INCREASE OF CATALYST B-6 DURING CARBURIZATION

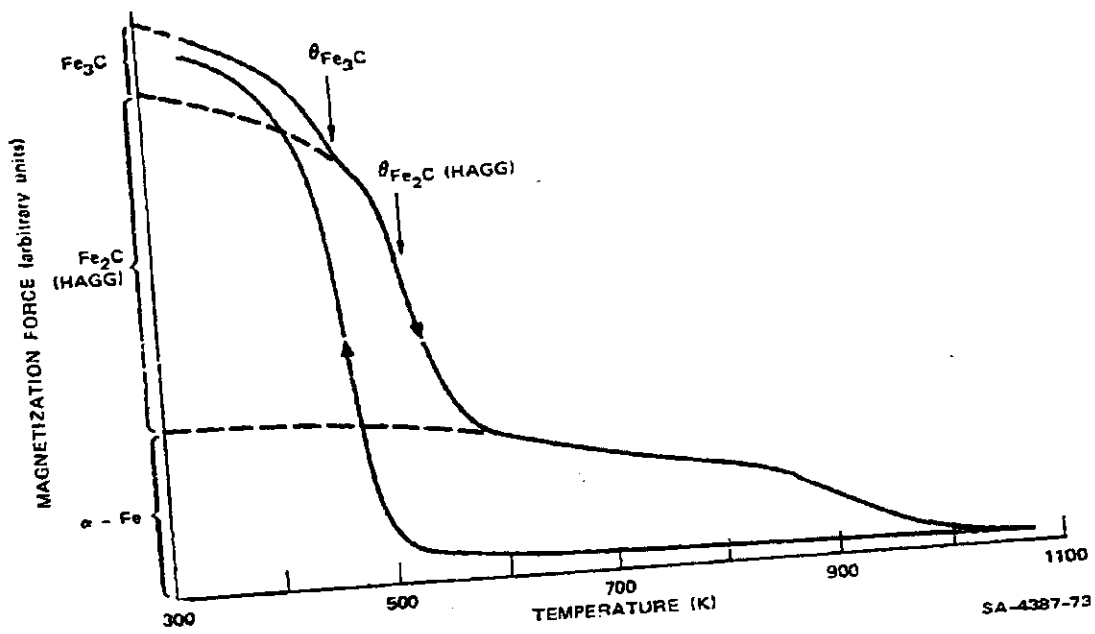


FIGURE 5-4 TYPICAL THERMOMAGNETIC ANALYSIS (TMA) OF CARBURIZED IRON FISCHER-TROPSCH CATALYST B-6

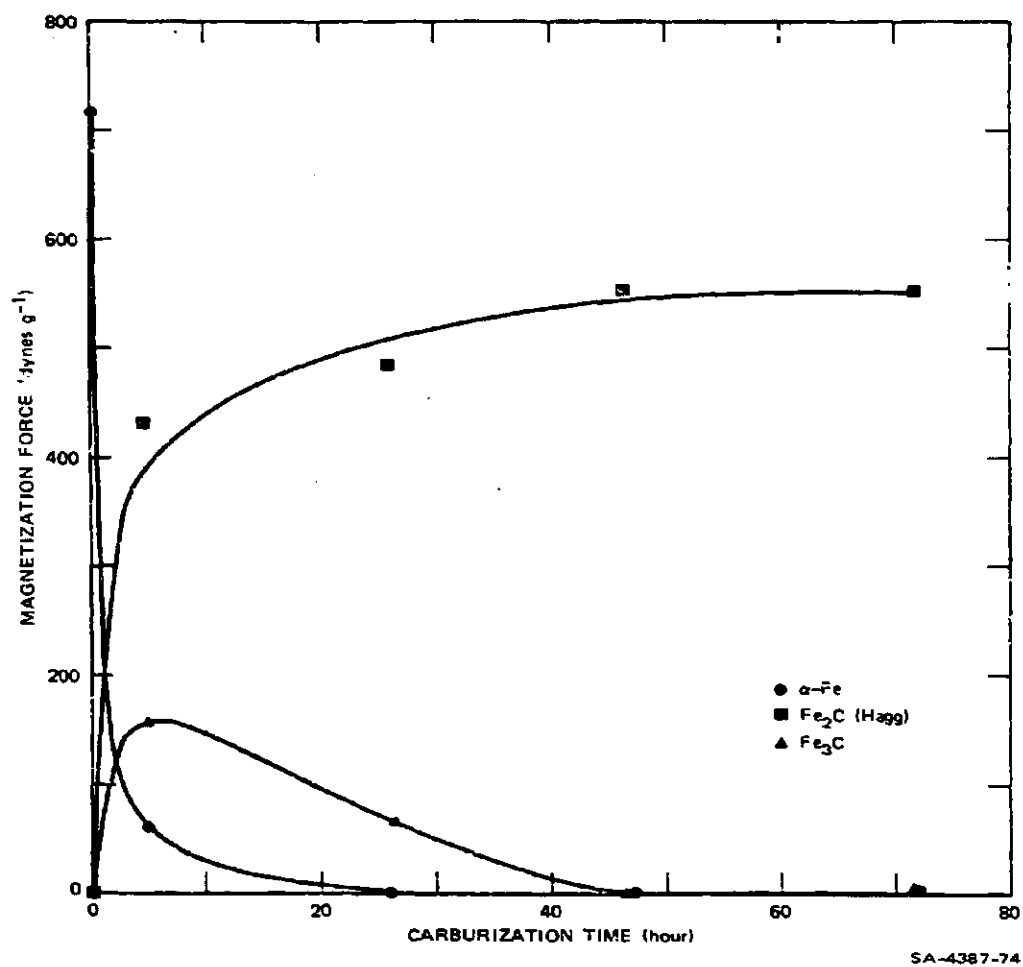


FIGURE 5-5 FERROMAGNETIC PHASES IN CATALYST B-6 DURING CARBURIZATION H_2/CO (3/1) at 1 atm; for temperature see Figure 5-1.

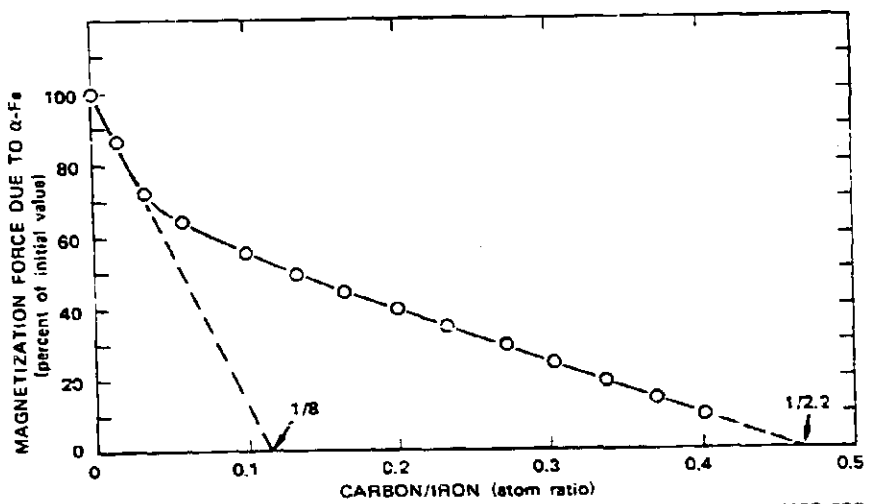
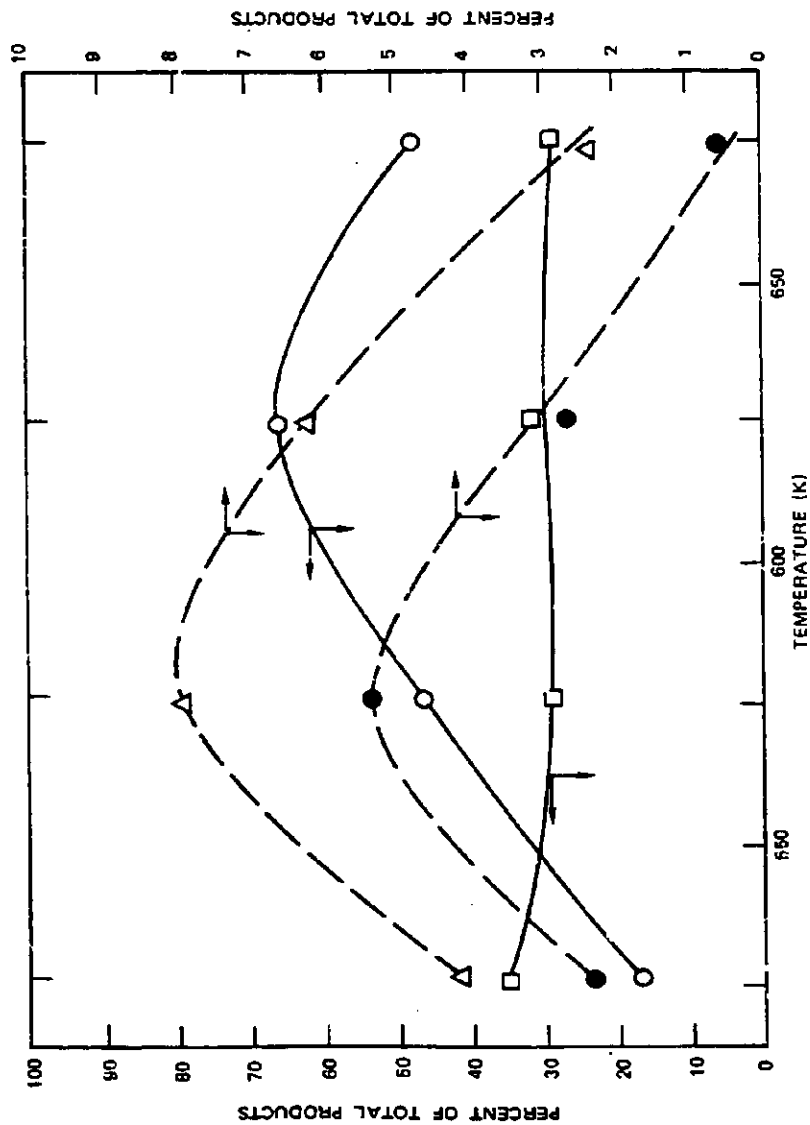


FIGURE 5-6 Magnetization force due to α -Fe as a function of carbon/iron ratio during carburization of reduced catalyst B-2 at 598 K

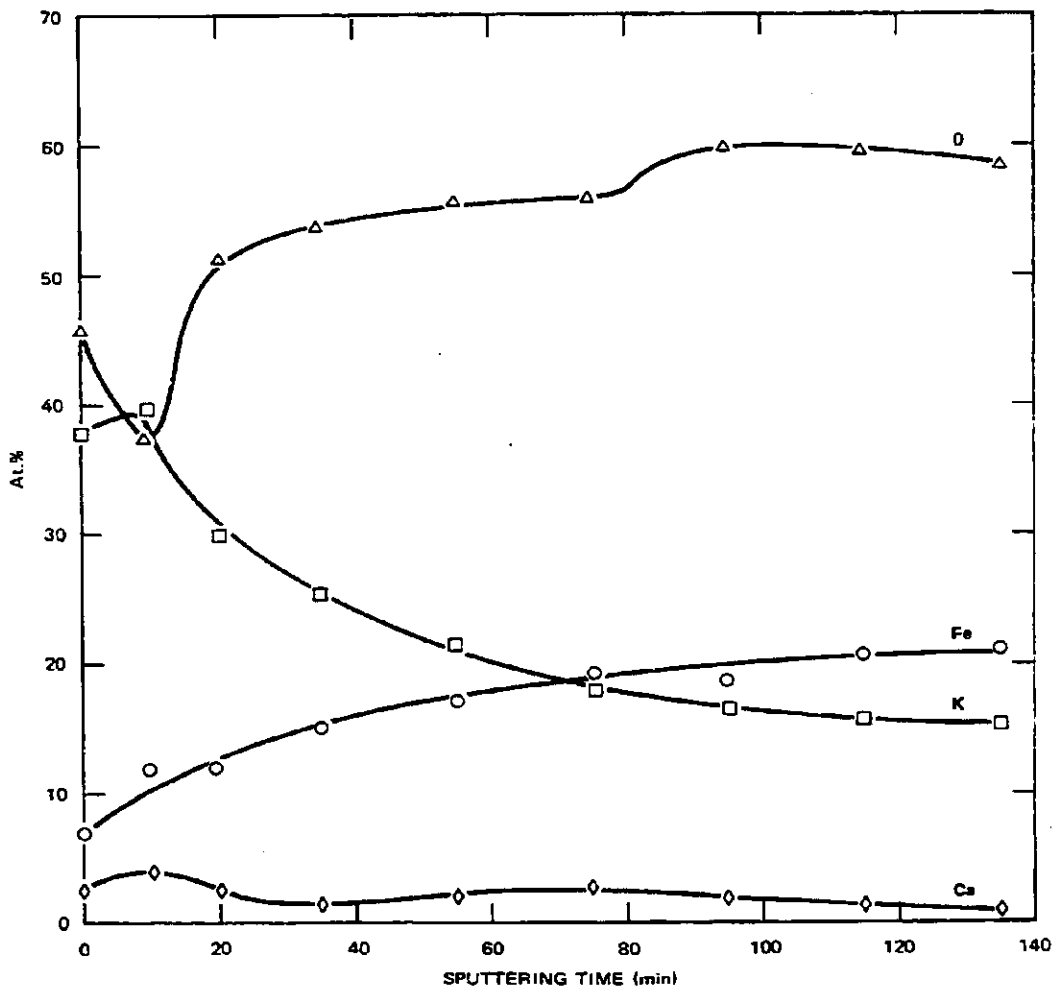


SA-4387-34

FIGURE 5-7 PRODUCT DISTRIBUTION AS A FUNCTION OF TEMPERATURE, CATALYST B-6 CARBURIZED AT 673 K IN H₂/CO = 3 AT 1 atm.

Feed gas: H₂/CO = 3/1; flow rate: 20 cm³/min, CO consumed = 100%.

○ CH₄; □ CO₂; △ C₂H₆; ● C₃H₈



SA-4387-45

FIGURE 5-8 DEPTH PROFILE OF FRESH CATALYST B-6

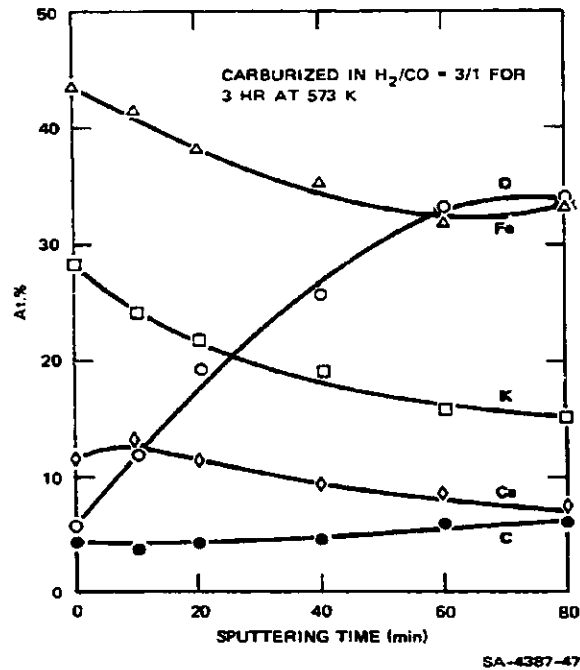
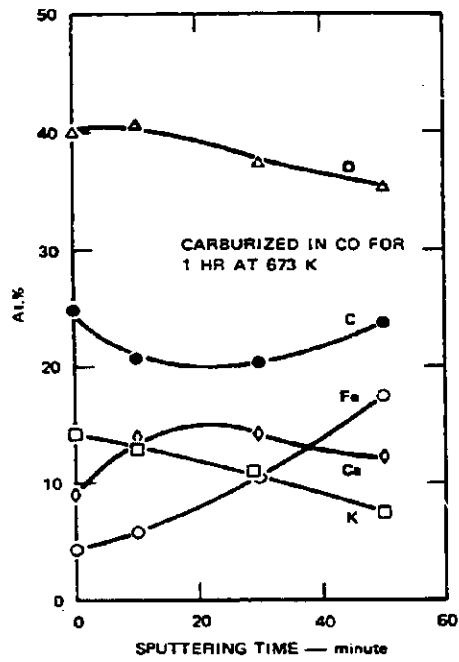
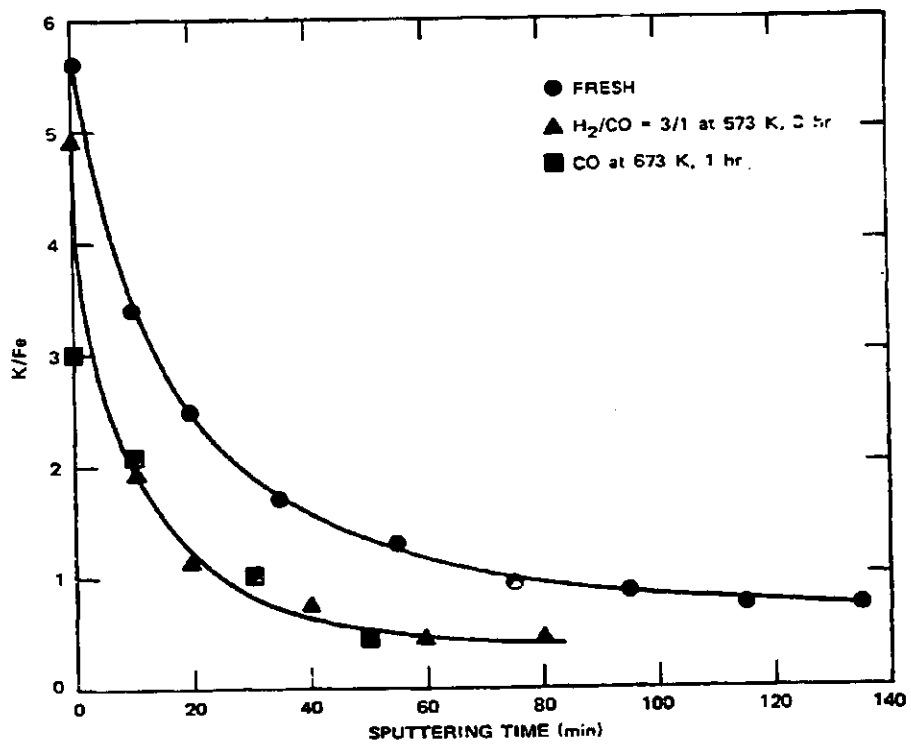


FIGURE 5-9 DEPTH PROFILES OF CARBURIZED CATALYST B-6



SA-4387-51

FIGURE 5-10 RELATIVE DEPTH DISTRIBUTION OF POTASSIUM FOR CATALYST B-6